

Document downloaded from:

<http://hdl.handle.net/10251/124294>

This paper must be cited as:

Carbonell Alcaina, C.; Alvarez Blanco, S.; Bes-Piá, M.; Mendoza Roca, JA.; Pastor Alcañiz, L. (2018). Ultrafiltration of residual fermentation brines from the production of table olives at different operating conditions. *Journal of Cleaner Production*. 189:662-672.  
<https://doi.org/10.1016/j.jclepro.2018.04.127>



The final publication is available at

<http://doi.org/10.1016/j.jclepro.2018.04.127>

Copyright Elsevier

Additional Information

1 **Ultrafiltration of residual fermentation brines from the production of table olives**  
2 **at different operating conditions**

3  
4 Carlos Carbonell-Alcaina<sup>1</sup>, Silvia Álvarez-Blanco<sup>1,2</sup>, María Amparo Bes-Piá<sup>1,2</sup>, José  
5 Antonio Mendoza-Roca<sup>1,2</sup>, Laura Pastor-Alcañiz<sup>3</sup>

6  
7 <sup>1</sup>*Research Institute for Industrial, Radiophysical and Environmental Safety (ISIRYM),*  
8 *Universitat Politècnica de València, C/Camino de Vera s/n, 46022 Valencia, Spain.*

9 <sup>2</sup>*Department of Chemical and Nuclear Engineering, Universitat Politècnica de*  
10 *València, C/Camino de Vera s/n, 46022 Valencia, Spain*

11 <sup>3</sup>*Depuración de Aguas del Mediterráneo (DAM), Avda. Benjamin Franklin, 21, Parque*  
12 *Tecnológico, 46980 Paterna (Valencia)*

13  
14 \*Corresponding author: Carlos Carbonell-Alcaina

15 E-mail addresses: carcaral@upvnet.upv.es

16 Phone: +34 963879630

17 Fax: +34 96 3877639

18  
19 **Abstract**

20  
21 The membrane process of ultrafiltration (UF) has been investigated as a pretreatment  
22 previous to the further recovery and concentration of phenolic compounds from residual  
23 table olives fermentation brines. Two UF membranes were tested: a permanently  
24 hydrophilic polyethersulfone (PES) membrane with a molecular weight cut-off (MWCO)  
25 of 30 kDa and a PES membrane with a MWCO of 5 kDa. Transmembrane pressure and

26 crossflow velocity were varied from 1 to 3 bar and from 2.2 to 3.7 m·s<sup>-1</sup>, respectively.  
27 The best membrane in terms of permeate flux and selectivity was that with MWCO of 5  
28 kDa and the best operating conditions were transmembrane pressure of 3 bar and  
29 crossflow velocity of 2.2 m·s<sup>-1</sup>. In these conditions permeate flux was 21.6 L·h<sup>-1</sup>·m<sup>-2</sup>,  
30 while the rejection of COD and phenolic compounds were 50.0% and 21.9%, respectively  
31 and the removal of color and turbidity was almost complete. In addition, an alkaline  
32 cleaning protocol was proposed, which was effective to restore the initial permeability  
33 of the selected membrane.

34

35 *Keywords:* Ultrafiltration; polyethersulfone membranes; table olive fermentation brine  
36 wastewater; phenolic compounds.

37

## 38 **1. Introduction**

39

40 In the last years, there has been a growing interest in obtaining high added value  
41 compounds from renewable raw materials and wastes. Some of these compounds have a  
42 potential use in food, cosmetic and pharmaceutical industries. Among these compounds,  
43 those with antioxidant properties have generated great interest. These compounds,  
44 which are abundant in the Mediterranean diet in the form of vitamins C and E,  
45 carotenoids and phenolic compounds, have beneficial effects on human health  
46 (Sánchez-Moreno et al., 2006) (Zulueta et al., 2007) (Guedes et al., 2011).

47

48 Phenolic compounds are present especially in fruits and vegetables. Olive fruit, which is  
49 one of the bases of the Mediterranean diet, contains a great quantity of these  
50 compounds. The production of olive fruits amounted to 5,700 tonnes in the 2014/2015

51 crop season (International Olive Council, 2015). Olive fruits can be processed to obtain  
52 olive oil or treated to be consumed directly as table olives. The number of olive fruits  
53 dedicated to the production of olive oil has always been higher than those used to  
54 prepare table olives. However, in recent years, such numbers are tending to equalize.  
55 The total world production of table olives in 2014 was close to 2,600 tonnes.  
56 Approximately, 85% of the production takes place in the Mediterranean area, being  
57 Spain in 2014 the major producer (around 22.1% of the world production), followed by  
58 Turkey and Egypt (around 16.6% and 15.4% of the world production, respectively)  
59 (International Olive Council, 2015). According to the Spanish Ministry of Environment,  
60 it is estimated that 1.5 kilograms of wastewater are generated per each kilogram of table  
61 olives produced in Spain.

62

63 To be consumed as table olives, the olive fruits must be processed to reduce their  
64 bitterness. Three types of wastewater streams are mainly generated from this process,  
65 which consists of three steps: lye treatment with NaOH, lye washing and olive  
66 fermentation in brine (Sánchez Gómez et al., 2006). Each of these three steps  
67 approximately generates the same volume of wastewater. According to the Spanish  
68 Ministry of Environment, in Spain, per each kilogram of table olive produced, 0.5 kg of  
69 fermentation brine wastewater is obtained. This is the wastewater that has been  
70 considered to carry out this work. During the fermentation in brine, the lactic  
71 fermentation of the olives occurs, thus reducing the basic pH of the solution to a pH of  
72 about 4. The fermentation of sugars is almost complete. In this process, part of the  
73 phenolic compounds from the olive fruits (mainly oleuropein) solubilises into the acid  
74 solution (Soler-Rivas et al., 2000). In this solution, most of the phenolic compounds  
75 disappeared, while the concentration of hydroxytyrosol and tyrosol increased (Brenes et

76 al., 1995). This is due to the hydrolysis of the phenolic compounds like oleuropein, as  
77 an example, that hydrolyzed into hydroxytyrosol (Brenes et al., 1995).

78

79 Apart from the acid pH, the fermentation brine wastewater is also characterized by a  
80 high salt concentration (conductivity from 80 to 95  $\text{mS}\cdot\text{cm}^{-1}$ ) and high soluble chemical  
81 oxygen demand (COD), of 15000 to 30000  $\text{mgO}_2\cdot\text{L}^{-1}$ . Part of this organic matter  
82 corresponds to the phenolic compounds (these concentration varying from 1000 to 2000  
83  $\text{mg}$  of tyrosol equivalents $\cdot\text{L}^{-1}$ ) (García-García et al., 2011) (Ferrer-Polonio et al., 2014).  
84 The main phenolic compounds present in olive brine are hydroxytyrosol (HTY) and  
85 tyrosol (TY) and they show an outstanding antioxidant activity (Brenes et al., 1995)  
86 (Fendri et al., 2013). Nevertheless, the presence of these compounds in the wastewater  
87 represents one of the major problems for its treatment, primarily because they are hardly  
88 biodegradable and secondly because of their significant antimicrobial activity, which  
89 reduces the efficiency of the biological processes in wastewater treatment plants (WWTP)  
90 (Parinos et al., 2007). Besides, the high salt concentration can also have a negatively impact  
91 on the WWTP process as it causes activated sludge deflocculation (Woolard and Irvine,  
92 1994) (Kargı and Dinçer, 1999) (Reid et al., 2006) (Lefebvre and Moletta, 2006). On  
93 the other hand, if the organic matter and phenolic compounds are removed, the brine  
94 can be reused in the table olive fermentation process. In this perspective, the recovered  
95 phenolic compounds, due to their potential antioxidant properties, are an attractive  
96 ingredient for the food, cosmetic and pharmaceutical industries (Tripoli et al., 2005).

97

98 It is therefore of a great interest the recovery of these valuable compounds from the  
99 waste streams from fruits and vegetables processing. Historically, the treatment of the  
100 olive brine waste water has been based on the reduction or elimination of the organic

101 matter with the aim of its reuse in later stages of the processing, as in the packaging  
102 stage. To this end, the treatments that have been considered were ultrafiltration (UF)  
103 (Brenes et al., 1990), UF and active carbon (Garrido et al., 1992), biological treatment  
104 (Brenes et al., 2000) (Ferrer-Polonio et al., 2015), advanced oxidation (Rivas et al.,  
105 2003) and electro-coagulation (García-García et al., 2011).

106

107 Nevertheless, in the literature, there are some works dealing with the recovery of  
108 phenolic compounds from olive mill wastewater (OMW), generated during olive oil  
109 production. In some of these studies, membrane process have been proposed by several  
110 authors (Garcia-Castello et al., 2010) (Cassano et al., 2013) (Zirehpour et al., 2015).  
111 These works have shown that the combined utilization of ultrafiltration and  
112 nanofiltration (NF) processes for treating OMW is more effective than performing the  
113 separation in one single step (Paraskeva et al., 2007) (Garcia-Castello et al., 2010)  
114 (Cassano et al., 2013). In these combined processes, UF was applied as pretreatment for  
115 COD removal, as this membrane process is not able to separate low-molecular-weight  
116 compounds. Then, the UF permeate was treated by NF in order to obtain a permeate  
117 rich in phenolic compounds (Cassano et al., 2013). Also, reverse osmosis, osmotic  
118 distillation and vacuum membrane distillation were used to concentrate the phenolic  
119 compounds from the NF permeate (Paraskeva et al., 2007) (Coskun et al., 2010)  
120 (Zagklis et al., 2015) (Garcia-Castello et al., 2010). In these works, it was observed that  
121 the ultrafiltration membranes suffered severe fouling, whereas the fouling of the NF  
122 membranes was largely reduced when UF was used as pretreatment.

123

124 In spite of the number of works aimed to the recovery of the phenolic compounds from  
125 OMW, up to now there are very few studies in the literature where the phenolic

126 compounds are recovered from wastewaters resulting from table olive production. El-  
127 Abbassi et al., 2014, used UF as a pretreatment for a subsequent extraction process of  
128 phenolic compounds from table olive production wastewaters (El-Abbassi et al., 2014).  
129 They used a magnetically stirred unit and compared the results obtained at different pH  
130 values. The best results in terms of decolorization and COD removal were obtained at  
131 acidic pH values. Kiai et al., 2014, considered membrane distillation technology in the  
132 treatment of table olive wastewaters for the concentration of phenolic compounds and to  
133 obtain high quality water (Kiai et al., 2014).

134

135 In this work, membrane processes were used to recover phenolic compounds from the  
136 fermentation brine wastewater generated during Spanish-style green table olive  
137 processing. For this purpose, an integrated process that combines UF and NF was  
138 proposed. This work investigates the UF step as a pretreatment prior to the NF step.  
139 Two flat sheet UF membranes and different operating conditions were compared with  
140 the objective of reducing the presence of a great amount of total suspended solids (TSS)  
141 and soluble COD. Then, the UF permeate would be processed by NF in order to obtain  
142 a permeate stream enriched in phenolic compounds, with a low content of soluble COD.  
143 Therefore, the UF membrane should show a low rejection of phenolic compounds. In  
144 this work, the capability of the UF process to remove TSS and soluble COD with less  
145 phenolic compounds rejection from table olive wastewaters has been investigated in  
146 order to improve the performance of the subsequent NF process. Therefore, according to  
147 this objective, the operating conditions that maximize the phenolic compounds/COD  
148 ratio have been sought.

149

150 **2. Material and methods**

151

## 152 *2.1. Feed samples*

153

154 In the present work, different real samples of residual table olive fermentation brine  
155 were supplied by a table olive packing plant in Valencia region (Spain). Due to the high  
156 content of suspended solids observed in the residual wastewater, a previous filtration  
157 step with a polyester cartridge filter of 60  $\mu\text{m}$  pore size (CA-0202-00, model GT,  
158 HydroWater, Spain) was performed. The samples were stored at 5 °C.

159

## 160 *2.2. Analytical methods*

161

162 Regarding the analytical methods considered, each parameter was measured in triplicate  
163 and the average value was calculated.

164

165 The conductivity and the pH were measured with an EC-Meter GLP 31+ conductimeter  
166 and a GLP 21+ pH-meter (Crison, Spain), respectively, at room temperature (25 °C).

167 Turbidity was measured with a turbidimeter (D-112, DINKO, Spain) following the

168 UNE-EN ISO 7027 standard method. The color of the samples was determined from

169 absorbance readings at 440 and 700 nm using a DR600 spectrophotometer (Hach

170 Lange, Germany). The color value was calculated as the difference between the two

171 absorbance readings in 1 cm pathlength cells as described by (De Castro and Brenes,

172 2001).

173

174 The amount of TSS was determined from 25 mL samples by means of glass microfiber

175 filters (1.2  $\mu\text{m}$  pore size), according to UNE 77034 standard method. After the filtration



176 of the samples, the microfiber filters were dried at 105 °C for 2 h. The amount of TSS  
177 corresponded to the difference between the initial weight of the filter and its weight  
178 after being dried.

179

180 The concentration of chloride ions was determined with LCK311 kits, (Hach Lange,  
181 Germany) and soluble COD with LCK014, LCK114 and LCK614 kits (Hach Lange,  
182 Germany). The DR600 spectrophotometer (Hach Lange) was used. In order to  
183 determine the COD, the samples were diluted to avoid the interferences caused by the  
184 high chloride concentration. The concentration of sodium ions was determined with  
185 Sodium Cell Test in nutrient solutions for fertilization photometric method (Merck  
186 Millipore, Germany). A NOVA 30 Spectroquant photometer (Merck Millipore,  
187 Germany) was used for the measurements.

188

189 In order to determine total concentration of phenolic compounds, the samples were  
190 previously acidified to pH 2 with HCl, washed with hexane and submitted to a liquid–  
191 liquid extraction with ethyl acetate (El-Abbassi et al., 2011). The ethyl acetate extract  
192 was evaporated to dryness using an R-114 Rotavapor (BüchiLabortechnik AG,  
193 Switzerland) at 40 °C. Then, the residue was dissolved in methanol. Total phenolic  
194 compounds concentration was determined by means of the Folin-Ciocalteu method  
195 following the procedure described by (Singleton et al., 1999). A solution of sodium  
196 carbonate (Panreac, Spain) in water (20% w/v) and the Folin and Ciocalteu's reagent  
197 (Sigma Aldrich, USA) were used. At the end of the procedure, the absorbance at 765  
198 nm ( $Abs_{765}$ ) was measured with the DR600 spectrophotometer. The results were  
199 expressed as milligrams of tyrosol equivalents per liter ( $\text{mg tyrosol eq}\cdot\text{L}^{-1}$ ). The relation  
200 obtained was  $\text{mg tyrosol eq}\cdot\text{L}^{-1} = 558.96 \cdot Abs_{765}$ , with  $R^2 = 0.996$ .

201

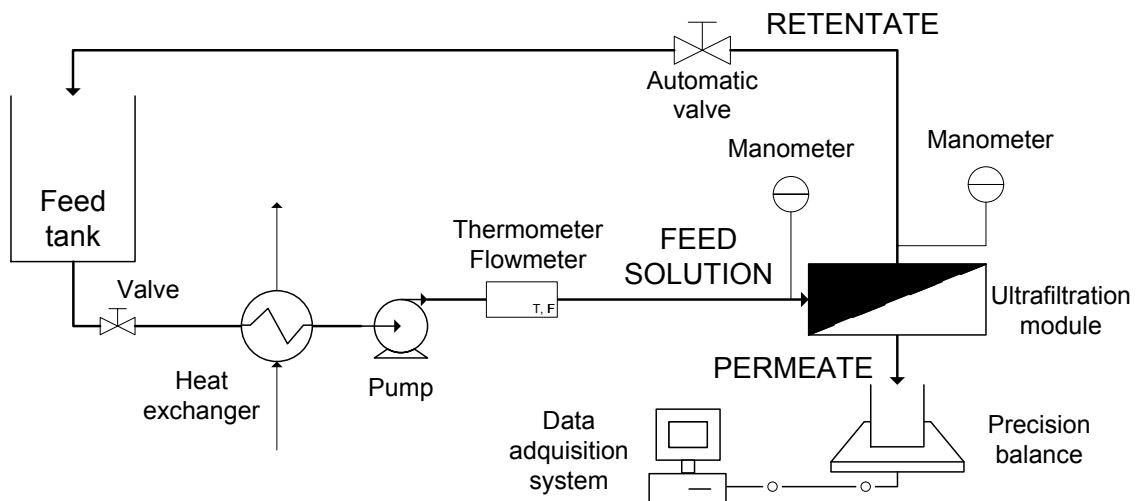
202 High performance liquid chromatography (HPLC) was used to determine the phenolic  
203 profile, and the concentration of tyrosol and hydroxytyrosol. The device was equipped  
204 with a PU-2089 Plus quaternary gradient pump (Jasco, Japan) and a MD2018 Plus  
205 Photodiode Array detector (Jasco, Japan). A Kinetex 5u C18 100A column  
206 (4.6×250mm, 5µm) (Phenomenex, USA) was used for the separation of the compounds.  
207 The operating conditions were the following: flow rate 1.5 mL·min<sup>-1</sup>, injected volume  
208 10.0 µL and wavelength UV detection 275 nm. The mobile phase was water/methanol  
209 (HPLC grade, VWR Chemicals, USA) with 1% v/v of glacial acetic acid (HPLC grade,  
210 Fisher Chemical, USA) in 30 min gradient. The gradient curve was 5% v/v of methanol  
211 for 1 minute, followed by a linear increase to 80% v/v over 25 min and return to 5% v/v  
212 of methanol over 2 min. An isocratic mobile phase of 5% v/v of methanol was passed  
213 through the column for 10 min before the next sample injection. The samples injected  
214 were prepared by the method developed by El-Abbassi et al. 2011. These samples were  
215 prepared so that they have a final concentration of 7 mg·mL<sup>-1</sup> in methanol. Calibration  
216 curves of TY (Sigma Aldrich, USA) and HTY (Sigma Aldrich, USA) were prepared at  
217 different concentrations ( $C_{TY}$  and  $C_{HTY}$ , respectively). Hydroquinone (Sigma Aldrich,  
218 USA) at 0.5 mg·mL<sup>-1</sup> concentration ( $C_{HQ}$ ) was used as internal standard. The calibration  
219 curves obtained were the following:  $A_{TY}/A_{HQ} = 1.0117 \cdot C_{TY}/C_{HQ}$  ( $R^2 = 0.9999$ ) and  
220  $A_{HTY}/A_{HQ} = 1.0117 \cdot C_{HTY}/C_{HQ}$  ( $R^2 = 0.9967$ ). Where  $A_{TY}$  is de peak area corresponding  
221 to tyrosol,  $A_{HTY}$  is de peak area corresponding to hydroxytyrosol and  $A_{HQ}$  is de peak area  
222 for hydroquinone.

223

### 224 2.3. Ultrafiltration

225

226 Fig. 1 shows the diagram of the ultrafiltration plant. This plant was automated, being the  
 227 cross flow velocity (CFV), the transmembrane pressure (TMP) and the temperature  
 228 automatically regulated. The plant was equipped with an UF module for a single flat  
 229 sheet membrane (Rayflow, Orelis, France) with a total active surface of 0.0125 m<sup>2</sup>. Two  
 230 ultrafiltration polyethersulfone membranes from Microdyn Nadir (Germany) were  
 231 tested: the permanently hydrophilic UH030 membrane and the UP005 membrane, with  
 232 a molecular weight cut-off (MWCO) of 30 and 5 kDa, respectively.  
 233



234  
 235  
 236

**Fig. 1.** Schematic diagram of the ultrafiltration plant.

237 The CFV was varied from 2.2 to 3.7 m·s<sup>-1</sup> and the TMP from 1 to 3 bar. The  
 238 ultrafiltration tests lasted 2.5 h, time enough to reach steady state permeate flux.  
 239 Temperature was kept constant at 25 °C by a heat exchanger connected to tap water.  
 240 The runs were performed according to a design of experiments with two factors (CFV  
 241 and TMP) for each membrane. The objective of these tests was to study the evolution of  
 242 the permeate flux with time, the stationary permeate fluxes achieved and the rejection of  
 243 COD and phenolic compounds by the membranes. Permeate flux was gravimetrically  
 244 measured with a Kern PKP precision balance (Kern, Germany) and the collected data

245 were recorded with a data acquisition system. During each test, retentate and permeate  
246 were recycled back to the feed tank in order to keep constant feed concentration.

247

248 The membranes separation efficiency was evaluated by calculating the removal of color,  
249 turbidity and conductivity by means of equation (Eq. 1) and the rejection of COD and  
250 phenolic compounds according to equation (Eq. 2).

251

$$E_i(\%) = \left(1 - \frac{V_{Pi}}{V_{Fi}}\right) \cdot 100 \quad (\text{Eq. 1})$$

252

$$R_j(\%) = \left(1 - \frac{C_{Pj}}{C_{Fj}}\right) \cdot 100 \quad (\text{Eq. 2})$$

253

254 where  $E_i$  is the elimination efficiency of parameter  $i$  (color, turbidity or conductivity),  
255  $V_{Pi}$  is the value of parameter  $i$  in the permeate,  $V_{Fi}$  is the value of parameter  $i$  in the feed  
256 solution,  $R_j$  is the rejection of parameter  $j$  (COD or phenolic compounds),  $C_{Pj}$  is the  
257 concentration of parameter  $j$  in the permeate and  $C_{Fj}$  is the concentration of parameter  $j$   
258 in the feed solution.

259

260 At the end of each ultrafiltration run, the membranes were cleaned. The cleaning  
261 protocol proposed was the following (C1): rinsing the membranes with osmotic water  
262 for 9 min, chemical cleaning with a concentrated basic solution of NaOH (pH 11)  
263 (Panreac, Spain) for 5 min with recirculation of the solution, rinsing with osmotic water  
264 for 9 min, chemical cleaning with a solution of citric acid (1% w/v) (Panreac, Spain) for  
265 5 min with recirculation of the solution and a final rinsing with osmotic water for 9 min.  
266 All of the cleaning steps were carried at a CFV of  $2.2 \text{ m}\cdot\text{s}^{-1}$  and room temperature. In

267 these conditions TMP was set to 0.6 bar. The membrane was considered to be cleaned if  
268 the hydraulic permeability after the cleaning step reached more than 95% of the initial  
269 one. If membrane hydraulic permeability was not recovered with this cleaning method,  
270 the temperature of chemical solutions and cleaning times were increased as follows: i)  
271 cleaning temperature was set at 35 °C for 15 min (C2), and ii) if membrane permeability  
272 remained unrecovered, temperature was set at 40 °C for 30 min (C3). The efficiency of  
273 the cleaning protocols was determined by comparing the hydraulic permeability of the  
274 new membrane with that of the cleaned membrane. After being cleaned, the membrane  
275 module was filled with osmotic water. The hydraulic permeability of the membrane was  
276 checked again before starting a new run.

277

### 278 **3. Results**

279

#### 280 *3.1. Characterization of the feed samples*

281

282 The main physicochemical characteristics of the residual olive fermentation brine  
283 wastewater are shown in Table 1. This wastewater is characterized by an acid pH (4.3),  
284 a high salt concentration and a high concentration of phenolic compounds (~ 1 g  
285 Tyrosol eq·L<sup>-1</sup>). This wastewater showed a high conductivity due to the presence of  
286 NaCl added in the fermentation step ( $73.8 \pm 13.1$  mS·cm<sup>-1</sup>). The residual water was  
287 yellow coloured due to the natural pigments contained in the olives. As it was  
288 explained, during lactic fermentation, the brine was enriched in phenolic compounds.  
289 As shown in Table 1, about half of the concentration of phenolic compounds  
290 corresponded to HYT and TY. The samples also showed a high concentration of TSS  
291 ( $759.7 \pm 642.5$  mg·L<sup>-1</sup>) and a high value of soluble COD ( $13.3 \pm 4.6$  g·L<sup>-1</sup>) and turbidity

292 (378.5 ± 136.0 NTU). Such data exhibited quite a large standard deviation (SD) (see  
 293 Table 1) owing to several factors, such as the different variety of olive fruits processed,  
 294 harvest-time and fermentation time (Pereira et al., 2006).

295

296 **Table 1.**

297 The main physicochemical characteristics of real samples from residual olive  
 298 fermentation brine, supplied by a table olive packing plant in Valencia region.

Parameter	Mean value	SD <sup>a</sup>
pH	4.3	± 0.3
Conductivity (mS·cm <sup>-1</sup> )	73.8	± 13.1
Color	0.564	± 0.111
Turbidity (NTU)	378.5	± 136.0
TSS <sup>b</sup> (mg·L <sup>-1</sup> )	759.7	± 642.5
Soluble COD <sup>c</sup> (mgO <sub>2</sub> ·L <sup>-1</sup> )	13295	± 4616
Cl <sup>-</sup> (mg·L <sup>-1</sup> )	39302	± 6689
Na <sup>+</sup> (mg·L <sup>-1</sup> )	55667	± 22485
Total phenolic compounds (mg Tyrosol eq·L <sup>-1</sup> )	998.8	± 474.7
Hydroxytyrosol (mg·L <sup>-1</sup> )	473.4	± 306.6
Tyrosol (mg·L <sup>-1</sup> )	71.7	± 41.1

299

300 <sup>a</sup>SD: Standard deviation; <sup>b</sup>TSS: Total suspended solids; <sup>c</sup>COD: chemical oxygen demand

301

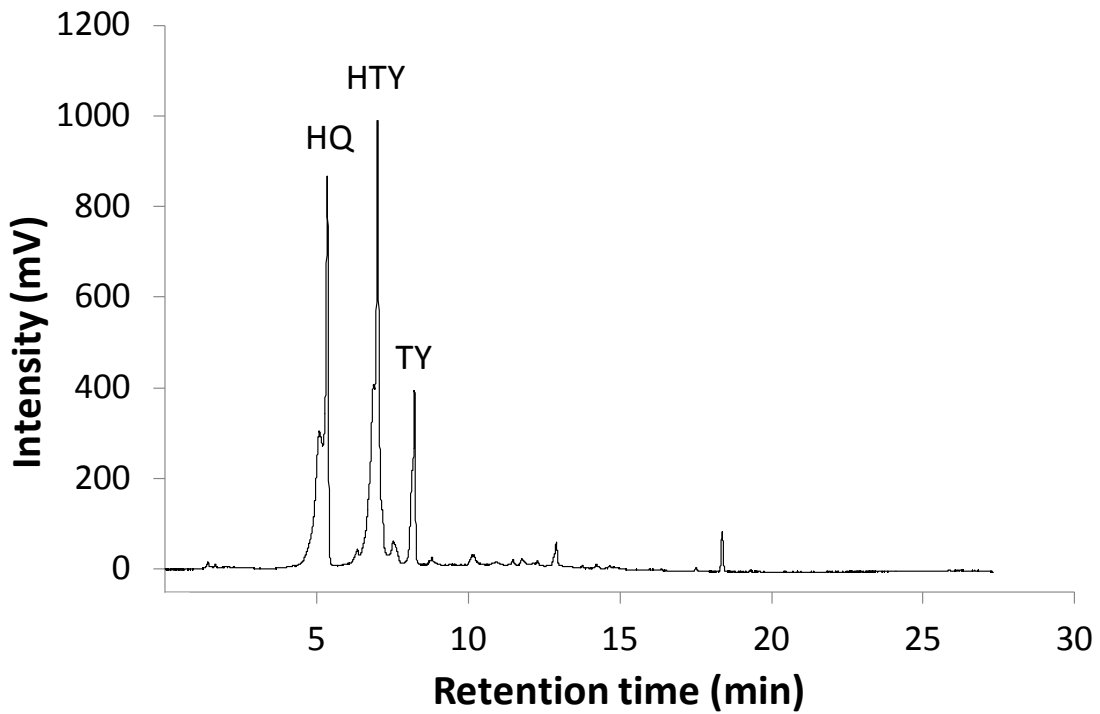
302 The preliminary filtration by means of the polyester cartridge filter reduced the amount  
 303 of organic matter and the turbidity without modifying the concentration of salts,  
 304 phenolic compounds and soluble COD. Due to the great variability in the content of  
 305 TSS (759.7 ± 642.5 mg·L<sup>-1</sup>), the samples that had the largest concentration of TSS  
 306 showed a greater percentage of elimination. Those samples with TSS greater than 1500  
 307 mg·L<sup>-1</sup> exhibited a reduction around 70 to 74%, while those with lowest TSS (between  
 308 550 and 350 mg·L<sup>-1</sup>) exhibited a reduction between 14 and 21%. Also, the reduction in  
 309 turbidity ranged between 8 and 39% depending on its initial value. The values of TSS  
 310 and turbidity in filtered samples were 530.1 ± 267.7 mg·L<sup>-1</sup> and 231.1 ± 61.5 NTU,  
 311 respectively. This preliminary filtration conducted to more homogeneous samples with  
 312 less SD.

313

314 Fig. 2 shows the phenolic compounds profile of one of the samples of the residual olive  
315 fermentation brine after being filtered. It can be observed that HTY and TY were the  
316 main phenolic compounds. They were present in all the analysed samples, while other  
317 phenolic compounds were not present in all of them. The results were similar to those  
318 obtained by other authors (Brenes et al., 1995) (Fendri et al., 2013) (Ferrer-Polonio et  
319 al., 2015), who reported that, for Spanish-style green olives, these compounds are those  
320 mainly present in residual wastewaters. However, other phenolic compounds showed  
321 lower concentrations as they gradually disappear during the fermentation stage. The  
322 concentrations of HTY and TY obtained by HPLC at the above described conditions  
323 were  $473.36 \pm 306.61 \text{ mg}\cdot\text{L}^{-1}$  and  $71.70 \pm 41.14 \text{ mg}\cdot\text{L}^{-1}$ , respectively, reported in Table  
324 1. The concentration of these compounds in the different samples was quite variable,  
325 depending on the olive fruit variety (Kiai and Hafidi, 2014) and the duration of the  
326 fermentation process (Ryan et al., 1999).

327

328



329

330

**Fig. 2.** HPLC phenolic compounds profile for a sample of the residual olive fermentation brine after being filtered.

331

332

333

### 3.2. Ultrafiltration step

334

335

Fig. 3 shows the values of permeate flux obtained when osmotic water was ultrafiltered

336

with both membranes, respectively, at different TMPs. From the observed linear

337

relationship between osmotic water permeate flux ( $J$ ) and TMP ( $\Delta P$ ), the hydraulic

338

permeability ( $K$ ) of both membranes can be calculated by means of the Darcy's

339

equation (Eq. 3):

340

$$J = K \cdot \Delta P = \frac{\Delta P}{\mu \cdot R_m} \quad (\text{Eq. 3})$$

341

342

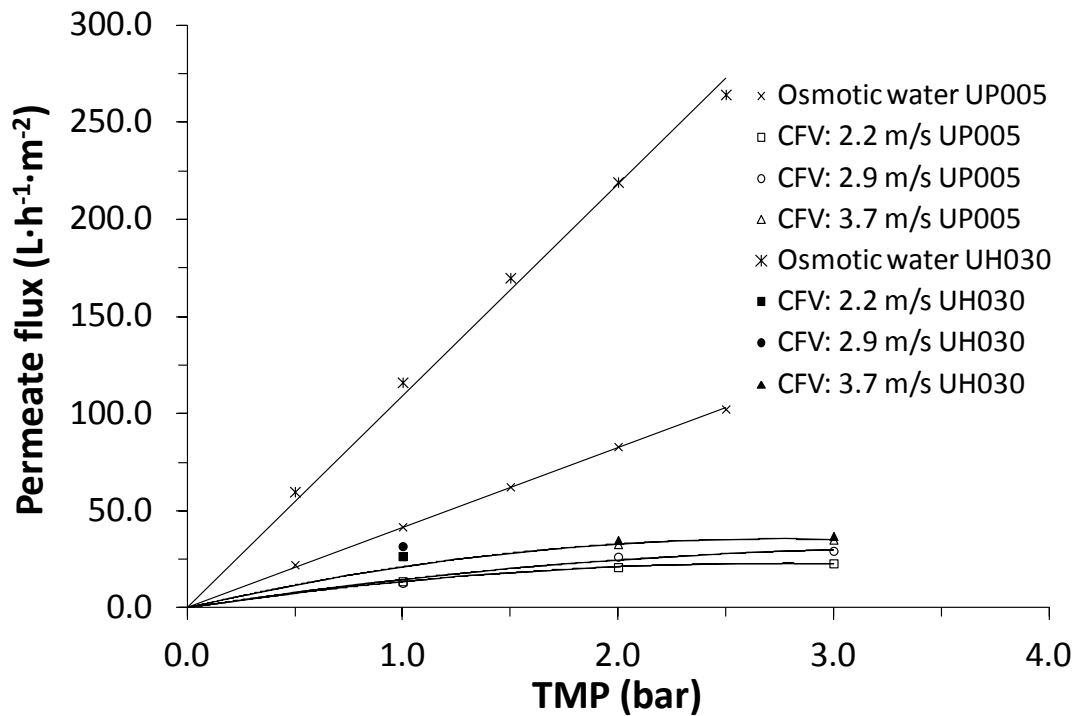
In this equation  $\mu$  and  $R_m$ , respectively, represent the viscosity of the permeate and the

343

intrinsic membrane resistance. By fitting osmotic water permeate flux at 25 °C against



344 the TMP, it was possible to estimate the following hydraulic permeability for the UP005  
 345 and UH030 membranes tested:  $45.48 \pm 4.01$  and  $95.84 \pm 10.87 \text{ L}\cdot\text{h}^{-1}\cdot\text{m}^{-2}\cdot\text{bar}^{-1}$ ,  
 346 respectively ( $R^2$  higher than 0.999 for the UP005 membrane and higher than 0.993 for  
 347 the UH030 membrane).  
 348



349 **Fig. 3.** Permeate flux in the ultrafiltration of osmotic water and residual brine at  
 350 different operating conditions for both UP005 and UH030 membranes.  
 351  
 352

353 Fig. 3 also shows the steady state permeate flux when the residual brine was  
 354 ultrafiltered with both membranes. Permeate flux was found to tend to an asymptotic  
 355 value, quite lower than the osmotic water permeate flux whatever the operating  
 356 conditions tested and for the both membranes used. This trend is indicative of severe  
 357 membrane fouling (Field and Pearce, 2011). Also, indicates that all the operating  
 358 conditions considered in this study were in the critical flux area (Bacchin et al., 2006).  
 359

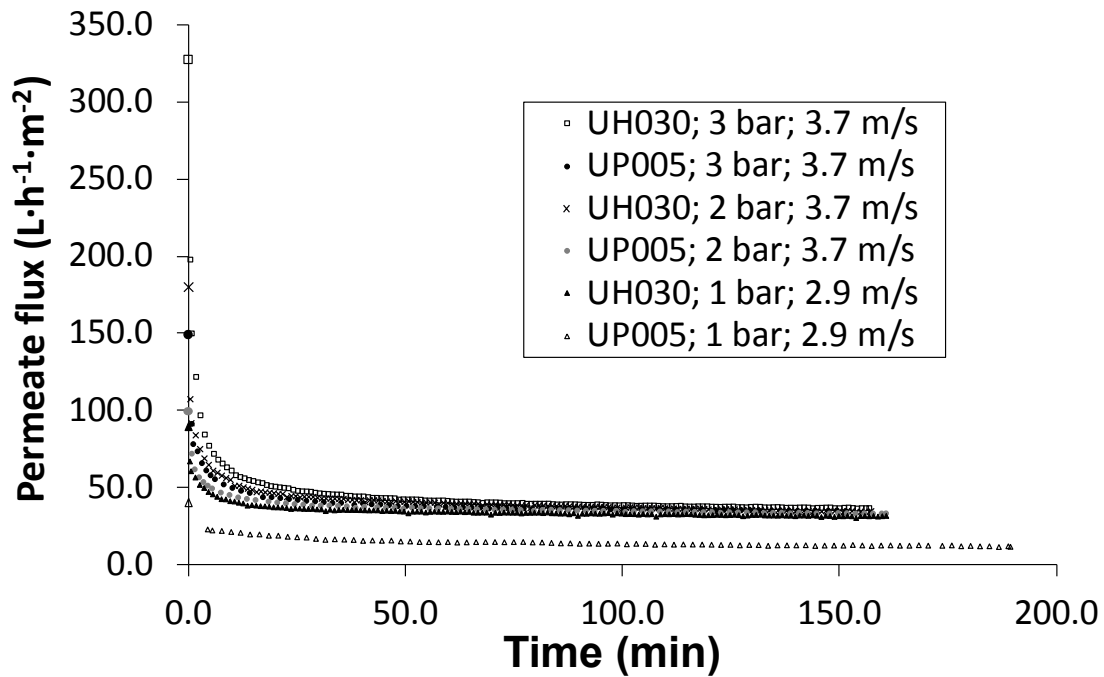
360 When the steady state permeate flux for both membranes is compared, it can be  
361 observed that at 1 bar the value reached was higher for the UH030 membrane ( $26.6 \text{ L}\cdot\text{h}^{-1}\cdot\text{m}^{-2}$   
362  $^1\cdot\text{m}^{-2}$  versus  $13.7 \text{ L}\cdot\text{h}^{-1}\cdot\text{m}^{-2}$  at  $2.2 \text{ m}\cdot\text{s}^{-1}$ ). At low pressure, the convective transport of  
363 solute molecules towards the membrane surface is less intense. Thus, concentration  
364 polarization and fouling are lower and the highest permeate flux is obtained with the  
365 membrane with higher MWCO. However, by increasing TMP to 2 and 3 bars the steady  
366 state permeate flux was similar for both membranes. This indicates that, at those TMPs,  
367 the fouling was greater for the UH030 membrane. Also, it can be observed that for the  
368 UP005 membrane the steady state permeate flux achieved at 1 bar was lower than the  
369 ones obtained at 2 and 3 bars, as it was expected. However, the differences between the  
370 permeate fluxes obtained at 2 and 3 bar for the same CFVs were lower. This fact  
371 indicates that these operating conditions are close to the limiting flux area (Bacchin et  
372 al., 2006) (Field and Pearce, 2011). On the other hand, for the UH030 membrane, it can  
373 be appreciated that the stationary permeate flux was similar for the three TMPs tested,  
374 clear indication that these operating conditions are in limiting flux area. In addition it  
375 was observed that, at the TMPs considered in this work, the CFV had a more significant  
376 influence on the stationary permeate flux than the TMP. The Reynolds numbers ( $Re$ ) for  
377 the CFVs considered, 2.2, 2.9 and  $3.7 \text{ m}\cdot\text{s}^{-1}$ , are 4990, 6578 and 8392, respectively,  
378 which correspond to turbulent flow regime ( $Re \geq 4000$ ) (Cheryan, 1998). The highest  
379 steady state permeate fluxes reached were  $37.1 \pm 0.2 \text{ L}\cdot\text{h}^{-1}\cdot\text{m}^{-2}$  for the UH030  
380 membrane at 3 bar and  $3.7 \text{ m}\cdot\text{s}^{-1}$  and  $35.2 \pm 0.1 \text{ L}\cdot\text{h}^{-1}\cdot\text{m}^{-2}$  for the UP005 membrane at  
381 the same conditions.

382

383 Fig. 4 displays the time course of permeate flux for both membranes under the operating  
384 conditions tested. In all the cases the evolution of permeate flux was similar, with a

385 severe decrease in the first minutes followed by a smooth gradual decline until a quasi-  
386 steady state permeate flux was reached (permeate flux decline was higher than 65% for  
387 both membranes). This evolution of permeate flux is typical in UF processes. According  
388 to several authors (Field et al., 1995) (Ho and Zydney, 2000), the great flux decline  
389 during the first minutes is due to a pore blocking phenomenon and the subsequent  
390 gradual slow flux decline is caused by the accumulation of foulant molecules on the  
391 membrane surface, forming a cake layer or a gel layer on it. Obviously, the initial  
392 permeate flux for the UH030 membrane was higher than that for the UP005 membrane  
393 at all the operating conditions tested. The greatest flux decrease for both membranes  
394 was observed at 3 bar, especially for the UH030 membrane (permeate flux decline close  
395 to 89%). At TMP equal to 2 and 3 bar, the permeate flux was similar for both  
396 membranes after an ultrafiltration time of 40 min. At TMP equal to 1 bar the permeate  
397 flux decreased rapidly too, but at that TMP the permeate flux was higher for the UH030  
398 membrane, as already noted in Fig. 3. The fast decline in the permeate flux in the first  
399 ultrafiltration times may be attributed to severe fouling caused by pore blocking  
400 (Carbonell-Alcaina et al., 2016). Also, the UH030 membrane suffered more severe  
401 fouling caused by pore blocking than the UP005 membrane during the first minutes of  
402 operation. The greatest fouling observed in the UH030 membrane may be due to the  
403 larger pore size. Also, Cassano et al. 2011, observed a strong adsorption of polyphenols  
404 on permanently hydrophilic PES membranes during the UF of OMW, that was probably  
405 due to polar interactions (electron donor-acceptor interactions, hydrogen bonds)  
406 between polyphenols and the membrane (Cassano et al., 2011). This degree of affinity  
407 between the phenolic compounds and PES membranes is enhanced the more  
408 hydrophilic the membrane is (Ulbricht et al., 2009).

409



410  
 411 **Fig. 4.** Evolution of permeate flux with time for UP005 and UH030 membranes at 25°C  
 412 and for certain transmembrane pressures and cross flow velocities.  
 413

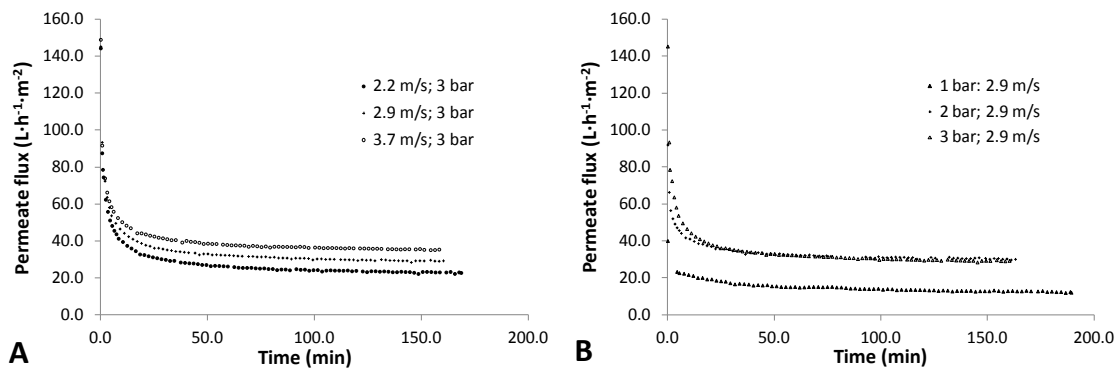
414 In a previous work (Carbonell-Alcaina et al., 2016), it was demonstrated that, when  
 415 residual brines from table olive packing plants were ultrafiltered, at the beginning of the  
 416 run the adsorption and concentration polarization resistance dominated, while at the  
 417 steady state the cake layer resistance was greater. Also, a rapid increase of the  
 418 adsorption and concentration polarization resistance ( $R_a$ ) was observed at the beginning  
 419 of the test. However, the increase of the cake layer resistance ( $R_{cf}$ ) with time was more  
 420 gradual, but it overcame the value of  $R_a$  before the steady state permeate flux was  
 421 reached.

422

423 Fig. 5a and 5b show the evolution of permeate flux with time under constant TMP (3  
 424 bar) at different CFVs and under constant CFV ( $2.9 \text{ m}\cdot\text{s}^{-1}$ ) at different TMPs,  
 425 respectively, for the UP005 membrane. The evolution of permeate flux was similar for  
 426 all the operating conditions, as it was previously commented. From Fig. 5a, at TMP  
 427 equal to 3 bar, by increasing CFV it was possible to increase the permeate flux. This

428 trend was also observed at TMP equal to 2 bar. However, at TMP equal to 1 bar the  
 429 effect of CFV on flux was lower, probably due to the lower concentration polarization  
 430 at that TMP. At a fixed CFV of 2.9 m·s<sup>-1</sup> (Fig. 5b), it can be appreciated that an increase  
 431 in the TMP from 1 to 2 bar caused an increment in the permeate flux. However, the  
 432 permeate flux was practically the same at 2 and 3 bar. At the highest TMP values tested  
 433 (2 and 3 bars), the limiting flux was reached (Fig. 3). Therefore, at those pressures, it  
 434 was not observed a significant dependence of permeate flux on TMP. This trend was  
 435 also noticed for the rest of the CFVs tested and for the UH030 membrane.

436



437

438

439

440

441

**Fig. 5.** Comparison of permeate flux evolution with time at 25°C for the UP005 membrane at a fixed TMP and different CFVs (A) and at a fixed CFV and different TMPs (B).

442

443

444

445

446

447

448

449

The residual fermentation brines from the production of table olives are complex mixtures of various solutes, apart from tyrosol and hydroxytyrosol, with unknown transport properties such as diffusivity. Among the solutes, polysaccharides and pectin can be found, which are usually related to the formation of a gel layer on the membrane surface (Mondal et al., 2012). This mixture of compounds also contains a high amount of total suspended solids. Mondal et al., 2012 proposed, for complex mixtures, a method to determine the mass transfer coefficient ( $k$ ) and quantify the concentration polarization factor ( $CP$ ). In this work the film theory and a correlation of the type  $Sh=Sh(Re,Sc)$  are

450 used to determine the effective diffusivity ( $D$ ) and the gel layer concentration ( $C_g$ ) of a  
451 mixture of various solutes from previously centrifuged Stevia plant extracts.

452

453 In the present work, in the area where the permeate fluxes have reached the limiting flux  
454 it has been considered that the gel layer was developed. If it is considered that solutes  
455 form a gel layer on the membrane surface and the permeate concentration is low, the  
456 classical film theory can be expressed as the following equation, where  $C_b$  is the bulk  
457 concentration:

458

$$J = k \cdot \ln \left( \frac{C_g}{C_b} \right) \quad (\text{Eq. 4})$$

459

460 According to Cheryan, 1998, for flat ultrafiltration membranes and turbulent flow ( $Re \geq$   
461 4000), the Sherwood number can be calculated by the following correlation:

462

$$Sh = \frac{k \cdot r}{D} = 0.023 \cdot Re^{0.8} \cdot Sc^{0.33} \quad (\text{Eq. 5})$$

463

464 Combining equations (Eq. 4) and (Eq. 5) the following expression is obtained:

465

$$J = \frac{D}{r} \cdot 0.023 \cdot Re^{0.8} \cdot Sc^{0.33} \cdot \ln \left( \frac{C_g}{C_b} \right) \quad (\text{Eq. 6})$$

466

467 Where the ratio  $C_g/C_b$ , is equivalent to a concentration polarization factor ( $CP$ ). In this  
468 expression the diffusivity and  $C_g$  have been considered to be constant and independent  
469 on the operating conditions (i.e. transmembrane pressure, crossflow velocity and feed  
470 concentration), while the mass transfer coefficient depends on the  $Re$  number. In order

471 to determine  $D$  and  $CP$ , an optimization method was employed. The method consisted  
472 in an initial guess for the values of these parameters in order to minimise the error  
473 between the experimental permeate flux and the theoretical permeate flux:

474

$$S = \frac{\sum_{i=1}^{N_{exp}} \left( \left[ \frac{J_{i,theoretical} - J_{i,exp}}{J_{i,exp}} \right]^2 \right)^{0.5}}{N_{exp}} \quad (Eq. 7)$$

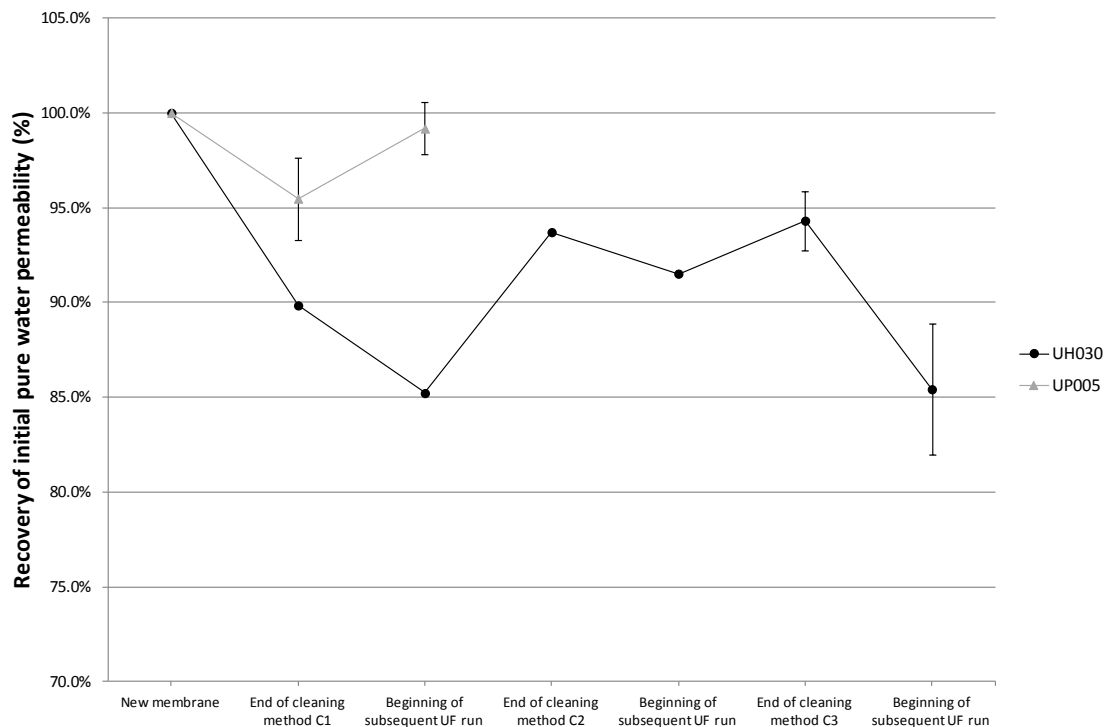
475

476 The mass transfer coefficients estimated were  $(1.99 \pm 0.02) \cdot 10^{-6} \text{ m}\cdot\text{s}^{-1}$ ,  $(2.40 \pm 0.13)$   
477  $\cdot 10^{-6} \text{ m}\cdot\text{s}^{-1}$  and  $(2.82 \pm 0.16) \cdot 10^{-6} \text{ m}\cdot\text{s}^{-1}$  for 2.2, 2.9 and  $3.7 \text{ m}\cdot\text{s}^{-1}$ , respectively. The  
478 effective diffusivity estimated was  $9 \cdot 10^{-13} \text{ m}^2\cdot\text{s}^{-1}$ , and  $CP$  varied from 19.0 to 40.0  
479 depending on feed concentration ( $S < 0.046$ ).

480

481 After each run, the membranes were cleaned following the procedures previously  
482 described. Fig. 6 displays the average recovery of pure water permeability for the two  
483 membranes tested after the cleaning process. As regarding the UP005 membrane, the  
484 cleaning method C1 resulted to be sufficient to achieve a permeability recovery greater  
485 than 95% for all the ultrafiltration tests performed at the different operating conditions  
486 tested. The hydraulic permeability of the UP005 membrane was newly checked before  
487 to start a new run. After a certain time period membrane submersion in osmotic water  
488 the hydraulic permeability increased, this resulting in an average permeability recovery  
489 greater than 99% for all the runs. However, the cleaning method C1 was not so efficient  
490 to recover the initial hydraulic permeability of the UH030 membrane. Thus, methods  
491 C2 and C3 were in sequence applied. As it is shown in Fig. 6, even after applying the  
492 C3 cleaning procedure, the initial hydraulic permeability of the UH030 membrane was  
493 not recovered. As it already noted, the fouling of this membrane was quite severe and its

494 fouling layer appeared to be more difficult to remove. Probably this membrane suffered  
 495 a greater irreversible fouling (Field and Pearce, 2011). Also, the roughness of such  
 496 membrane was greater than that of the UP005 membrane (Luján-Facundo et al., 2015).  
 497 The greater the membrane roughness the more severe fouling is and the fouling layer  
 498 can be more difficultly removed from the membrane surface (Vatanpour et al., 2014).  
 499 Despite the fact that the UH030 membrane is more hydrophilic than the UP005 one, its  
 500 fouling resulted to be more severe and the cleaning protocol used less effective. The  
 501 greater pore size of this membrane should have favoured fouling due to internal pore  
 502 blocking. This type of fouling was not only difficultly removed by means of the  
 503 cleaning protocols used, but also the membrane hydraulic permeability tending to  
 504 decrease became more persistent after membrane submersion in osmotic water. As it  
 505 can be observed in Fig. 6, for the UH030 membrane, the hydraulic permeability  
 506 recovery decreased after a certain time period submerged in osmotic water.  
 507



508 **Fig. 6.** Average recovery of initial pure water permeability for both membranes after the  
 509 different cleaning processes. The average permeability recovery shown was calculated  
 510



511 as the mean of recovery for all the runs performed at different operating conditions with  
 512 each membrane, respectively.

513

514 Table 2 shows the removal of salts, turbidity and colour, and the rejection of soluble  
 515 COD and phenolic compounds, by both membranes, as estimated by equations 1 and 2.

516 As it can be observed, the elimination of turbidity was greater than 99% for all the  
 517 operating conditions tested and both membranes. In all the runs, the permeate turbidity  
 518 was lower than 1.4 NTU.

519

**Table 2.** Removal of salts, colour and turbidity, and rejection of soluble COD and phenolic compounds, for the different operating conditions and for both ultrafiltration membranes.

Operating conditions		UP005 membrane					UH030 membrane				
TMP <sup>a</sup> (bar)	CFV <sup>b</sup> (m·s <sup>-1</sup> )	Removal of salts (%)	Removal of colour (%)	Removal of turbidity (%)	Rejection of soluble COD <sup>c</sup> (%)	Rejection of phenolic compounds (%)	Removal of salts (%)	Removal of colour (%)	Removal of turbidity (%)	Rejection of soluble COD <sup>c</sup> (%)	Rejection of phenolic compounds (%)
1	2.2	7.0	66.4	99.7	9.4	11.7	0	79.1	99.8	3.2	0.2
	2.9	3.1	67.1	99.9	16.0	2.8	0	78.9	99.8	0.7	0.0
2	2.2	6.6	66.1	99.7	11.8	-0.8	-	-	-	-	-
	2.9	5.6	78.7	100.0	18.9	-1.7	-	-	-	-	-
	3.7	11.5	76.8	99.6	34.0	17.9	3.2	81.5	99.6	6.6	1.8
3	2.2	8.1	82.8	99.4	50.0	21.9	-	-	-	-	-
	2.9	17.3	77.0	99.3	31.6	44.0	-	-	-	-	-
	3.7	33.7	78.8	99.3	13.5	34.5	0	81.9	99.7	21.5	24.5

520 <sup>a</sup>TMP: transmembrane pressure; <sup>b</sup>CFV: crossflow velocity; <sup>c</sup>COD: chemical oxygen demand

521

522 It can also be observed that the reduction of colour was slightly greater for the UH030  
 523 membrane. For this membrane, the removal of colour was similar for the different  
 524 operating conditions tested and it was around 80%. This membrane shows a greater  
 525 pore size, however, as it has been already commented, it exhibited greater fouling. Thus,  
 526 the fouling layer might contribute to increase the rejection of coloured compounds. In  
 527 the case of the UP005 membrane, colour rejection increased as TMP raised. The greater  
 528 rejection was observed for the operating conditions at which the limiting flux was  
 529 reached (2 and 3 bar). At those conditions colour rejection was similar to that observed  
 530 for the UH030 membrane.

531

532 Both membranes showed low salts removal, which is in agreement with the low  
533 molecular weight of NaCl. For the UH030 membrane it tended to zero at all the  
534 operating conditions tested, because of its greater pore size. For the UP005 membrane  
535 salts removal increased with TMP due to the greater fouling of the membrane as well as  
536 increased with CFV due to the reduction of the concentration at the membrane surface.  
537 The highest rejection of salts was 33.7% and it was achieved at 3 bar and  $3.7 \text{ m}\cdot\text{s}^{-1}$ . As  
538 show in Table 2, the rejection of COD was greater for the UP005 membrane, because of  
539 its smaller pore size. The rejection of COD depended as well on TMP and CFV. For the  
540 UP005 membrane, the removal of COD increased with CFV at 1 and 2 bar, as expected.  
541 However, at 3 bar, when the limiting flux was reached, the rejection of COD decreased  
542 with CFV. At this TMP, membrane fouling was severe, as already commented. Thus,  
543 the fouling layer could represent an additional resistance for the permeation of the  
544 solutes. At TMP equal to 3 bar and low CFVs the hydraulic resistance of the fouling  
545 layer was greater, as demonstrated by (Carbonell-Alcaina et al., 2016). This fact can be  
546 also observed from Fig. 5a, as permeate flux was observed to be lower at low CFV. The  
547 severe fouling observed at 3 bar and  $2.2 \text{ m}\cdot\text{s}^{-1}$  could be the reason for the higher  
548 rejection of COD (50%) observed in such conditions. By increasing CFV, the fouling  
549 layer might have been partially removed, thus reducing the COD rejection up to 13.5%  
550 at  $3.7 \text{ m}\cdot\text{s}^{-1}$ . For each CFV, the rejection of COD increased with TMP, except at  $3.7$   
551  $\text{m}\cdot\text{s}^{-1}$ . The increase in rejection with TMP can be attributed to the compaction of the  
552 fouling layer as TMP rises. As regarding the UH030 membrane, COD removal at TMP  
553 equal to 1 or 2 bar was very low. The greatest COD removal for this membrane  
554 occurred in the limiting flux area due to severe fouling.  
555

556 The rejection of phenolic compounds, was low for both membranes, due to the low  
557 molecular weight (MW) of the main phenolic compounds ( $MW_{HTY} = 154,16 \text{ g}\cdot\text{mol}^{-1}$ ;  
558  $MW_{TY} = 138,16 \text{ g}\cdot\text{mol}^{-1}$ ) present in the feed. The rejection of these compounds was  
559 slightly higher for the UP005 membrane due to the lower MWCO. The greatest  
560 rejection was observed at TMP equal to 3 bar for both membranes, due to greater  
561 fouling, while the lowest rejection was obtained at lower TMP and CFV values.

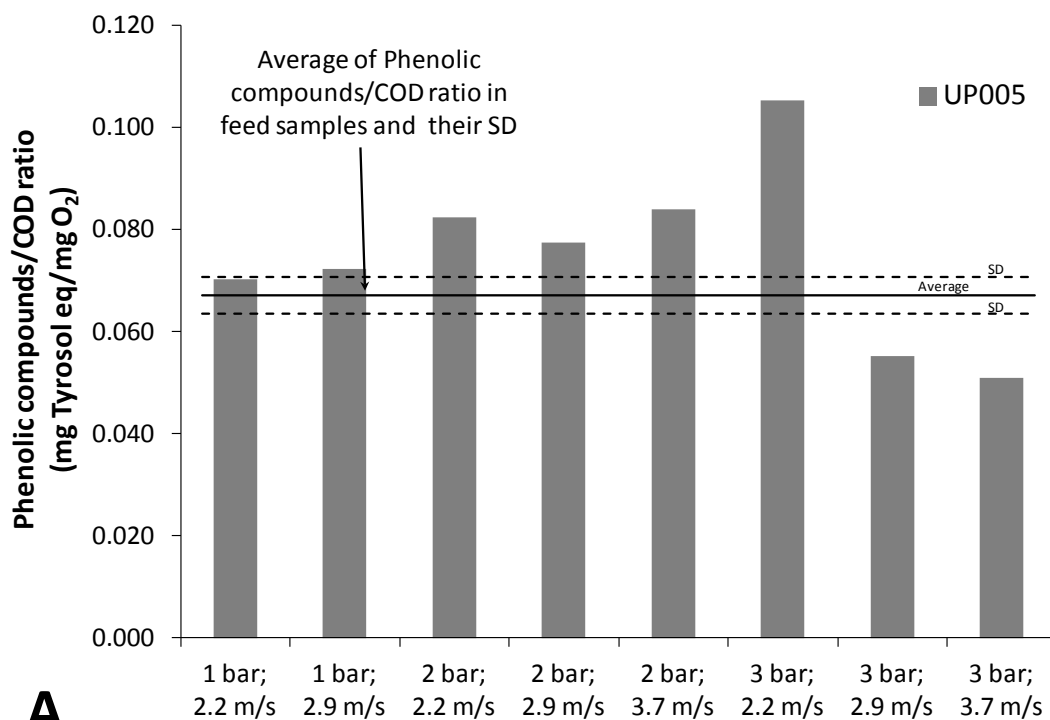
562

563 The different rejection for COD and phenolic compounds causes that the phenolic  
564 compounds/COD ratio in the permeate stream varies (Fig. 7a and 7b). As it can be  
565 observed in Fig. 7a, for the UP005 membrane the phenolic compounds/COD ratio  
566 increased in comparison with the feed solution, except at 3 bar and the highest cross  
567 flow velocities, due to the low COD rejection observed at those conditions. The greatest  
568 phenolic compounds/COD ratio in the permeate stream was achieved at 3 bar and 2.2  
569  $\text{m}\cdot\text{s}^{-1}$ . Thus, at these conditions the permeate stream showed the highest enrichment in  
570 phenolic compounds. However, for the UH030 membrane the phenolic  
571 compounds/COD ratio in the permeate practically did not vary in comparison with the  
572 feed (Fig. 7b). The same trend was observed by Cassano et al., 2011, when OMW were  
573 ultrafiltered by means of permanently hydrophilic membranes (Cassano et al., 2011).

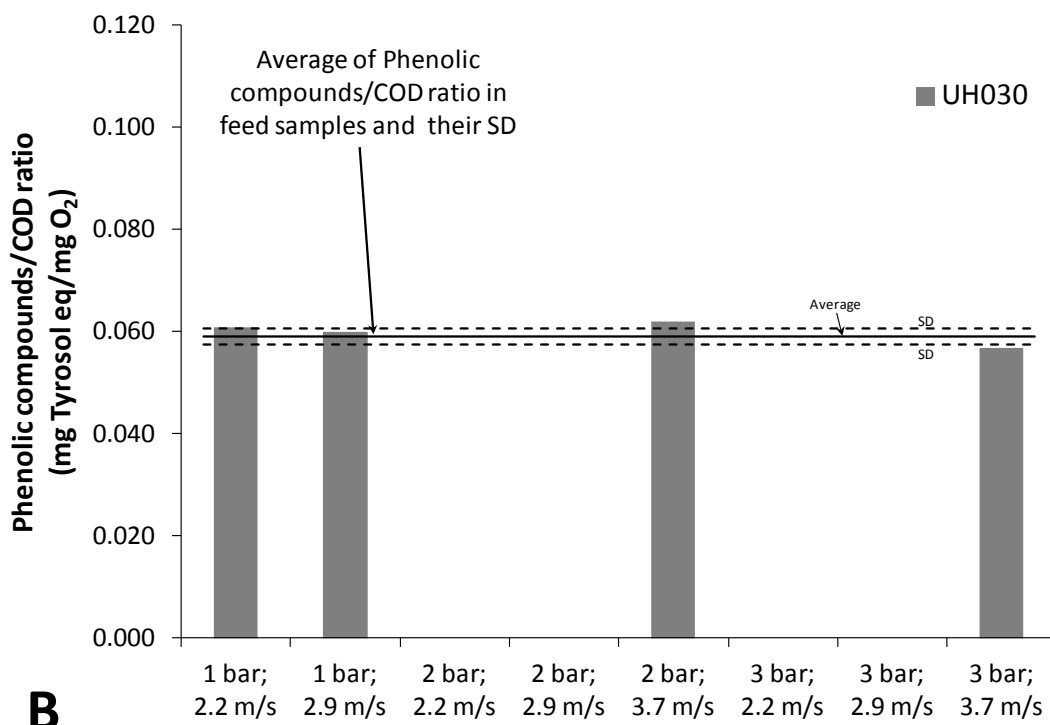
574

575 The objective of this work was to obtain a permeate stream enriched in phenolic  
576 compounds, with low values of turbidity, colour and soluble COD. Permeate flux was  
577 similar for both membranes. On the other hand, the UH030 membrane suffered greater  
578 fouling and the fouling layer was not completely removed after the cleaning process.  
579 Therefore, from this point of view, the UP005 membrane showed better results. This  
580 membrane also presented the largest rejection of DQO, being the rejection of phenolic

581 compounds low. Thus, UP005 membrane was chosen. The operating conditions selected  
 582 were a TMP of 3 bar and a CFV of  $2.2 \text{ m}\cdot\text{s}^{-1}$ . At those conditions the rejection of colour  
 583 and COD were the highest, while the rejection of phenolic compounds was low.  
 584



585



586  
 587  
 588

**Fig. 7.** Phenolic compounds/COD ratio in the permeate stream at different operating conditions and for UP005 (A) and UH030 (B) membranes. SD: standard deviation.

589

590 Table 3 shows the characterization of the permeate stream obtained when the residual  
591 brine was ultrafiltered with the UP005 membrane at the selected operating conditions.  
592 The permeate conductivity was slightly lower than that of the feed. The colour, turbidity  
593 and TSS of the samples were mostly removed. As it was previously commented, the  
594 value of COD in permeate was approximately 50% of that of the feed stream. At these  
595 conditions, the losses of phenolic compounds were around 21.9% with a final  
596 concentration of  $744.9 \pm 17.9 \text{ mg}\cdot\text{L}^{-1}$  Tyrosol eq. The rejection of HTY and TY was  
597 20.0% and 19.3%, respectively.

598

599

**Table 3.**

600

Characterization of ultrafiltration permeate obtained with the UP005 membrane at  
601 3 bar,  $2.2 \text{ m}\cdot\text{s}^{-1}$  and  $25^\circ\text{C}$ .

601

Parameter	Mean value	SD <sup>a</sup>
pH	4.1	$\pm 0.1$
Conductivity ( $\text{mS}\cdot\text{cm}^{-1}$ )	67.5	$\pm 0.3$
Color	0.098	$\pm 0.004$
Turbidity (NTU)	1.081	$\pm 0.035$
TSS <sup>b</sup> ( $\text{mg}\cdot\text{L}^{-1}$ )	0.0	$\pm 0.0$
Soluble COD <sup>c</sup> ( $\text{mg}\cdot\text{L}^{-1}$ )	7071.6	$\pm 59.9$
Total phenolic compounds ( $\text{mg}\cdot\text{L}^{-1}$ Tyrosol eq.)	744.9	$\pm 17.9$
Hydroxytyrosol ( $\text{mg}\cdot\text{L}^{-1}$ )	442.2	$\pm 6.1$
Tyrosol ( $\text{mg}\cdot\text{L}^{-1}$ )	66.3	$\pm 1.0$

602

<sup>a</sup>SD: Standard deviation; <sup>b</sup>TSS: Total suspended solids; <sup>c</sup>COD: chemical oxygen demand

603

604

#### 4. Conclusions

605

606 Permeate flux decreased fast with time during the first minutes of operation for both  
607 membranes at all the operating conditions tested. Therefore membrane fouling was  
608 severe. Although both membranes have different MWCO, the steady state permeate flux  
609 was similar and ranged between 20 and  $40 \text{ L}\cdot\text{h}^{-1}\cdot\text{m}^{-2}$  except for the UP005 membrane at  
610 1 bar. In this case permeate flux was much lower. At 2 and 3 bar the values of permeate  
611 flux were analogous, but they increased with CFV.

612

613 The alkaline cleaning protocol proposed was effective to restore the initial permeability  
614 of the UP005 membrane. However, it was not effective for the UP030 as it suffered  
615 more severe fouling.

616

617 At all the operating conditions examined both membranes were able to remove most of  
618 the colour and turbidity of the feed samples. Nevertheless, the rejection of COD and  
619 phenolic compounds varied with TMP and CFV. The greatest phenolic compounds/COD  
620 ratio (0.105 mg Tyrosol eq/mg O<sub>2</sub>) in permeate stream was obtained at 3 bar and 2.2  
621 m·s<sup>-1</sup> for the UP005 membrane. At these conditions COD and phenolic compounds  
622 rejection were 50.0% and 21.9%, respectively. As it is commented in the introduction  
623 section, a further treatment step, such as nanofiltration, is required for phenolic  
624 reclamation. The objectives of the UF step were to remove TSS and soluble COD with  
625 less phenolic compounds rejection in order to improve the performance of the  
626 subsequent NF process.

627

628 According to the results obtained, the ultrafiltration process carried out with the UP005  
629 membrane at the selected conditions can be considered as an efficient pretreatment for the  
630 subsequent recovery of polyphenols from table olive fermentation brine wastewaters.

631

### 632 **Acknowledgements**

633

634 The authors of this work wish to gratefully acknowledge the financial support of CDTI  
635 (Centre for Industrial Technological Development) depending on the Spanish Ministry  
636 of Science and Innovation (INNPRONTA program, ITP-20111020).

637

638 **Nomenclature**

639

640 *List of symbols*

641  $A_{HQ}$  peak area corresponding to hydroquinone

642  $A_{HTY}$  peak area corresponding to hydroxytyrosol

643  $A_{TY}$  peak area corresponding to tyrosol

644  $Abs_{765}$  Absorbance at 765 nm

645  $C_b$  bulk concentration

646  $C_{Fj}$  Concentration of parameter  $j$  in the feed solution

647  $C_g$  gel layer concentration

648  $C_{HQ}$  hydroquinone concentration

649  $C_{HTY}$  hydroxytyrosol concentration

650  $C_{Pj}$  Concentration of parameter  $j$  in the permeate solution

651  $CP$  concentration polarization factor

652  $C_{TY}$  tyrosol concentration

653  $D$  effective diffusivity

654  $E_i$  Elimination rate of parameter  $i$

655  $J$  Permeate flux

656  $k$  mass transfer coefficient

657  $K$  Hydraulic permeability

658  $R_a$  Resistance due to adsorption on membrane surface and inside its pores and  
659 concentration polarization

660  $R_{cf}$  Cake layer resistance

661  $Re$  Reynolds number

662	$R_j$	Rejection rate of parameter $j$
663	$R_m$	Intrinsic hydraulic resistance of the new membrane
664	$Sc$	Schmidt number
665	$Sh$	Sherwood number
666	$V_{Fi}$	Value of parameter $i$ in the feed solution
667	$V_{Pi}$	Value of parameter $i$ in the permeate solution
668	$\Delta P$	Transmembrane pressure
669	$\mu$	Viscosity of feed solution

670

671 *Abbreviations*

672

673	CFV	Crossflow velocity
674	COD	Chemical oxygen demand
675	C1	Cleaning protocol 1
676	C2	Cleaning protocol 2
677	C3	Cleaning protocol 3
678	HPLC	High performance liquid chromatography
679	HTY	Hydroxytyrosol
680	MW	Molecular weight
681	MWCO	Molecular weight cut-off
682	NF	Nanofiltration
683	NTU	Nephelometric turbidity unit
684	OMW	Olive mill wastewater
685	PES	Polyethersulfone
686	TMP	Transmembrane pressure



687 TSS Total suspended solids  
688 TY Tyrosol  
689 UF Ultrafiltration  
690 WWTP Wastewater treatment plants

691

## 692 **References**

693 Bacchin, P., Aimar, P., Field, R.W., 2006. Critical and sustainable fluxes: Theory,  
694 experiments and applications. *J. Memb. Sci.* 281, 42–69.  
695 doi:10.1016/j.memsci.2006.04.014

696 Brenes, M., García, P., Romero, C., Garrido, A., 2000. Treatment of green table olive  
697 waste waters by an activated-sludge process. *J. Chem. Technol. Biotechnol.* 75,  
698 459–463. doi:10.1002/1097-4660(200006)75:6<459::AID-JCTB234>3.0.CO;2-D

699 Brenes, M., Montaña, A., Garrido, A., 1990. Ultrafiltration of green table olive brines:  
700 Influence of some operating parameters and effect on polyphenol composition. *J.*  
701 *Food Sci.* 55, 214–217. doi:10.1111/j.1365-2621.1990.tb06055.x

702 Brenes, M., Rejano, L., Garcia, P., Sanchez, A., Garrido, A., 1995. Biochemical  
703 changes in phenolic compounds during Spanish-style green olive processing. *J.*  
704 *Agric. Food Chem.* 43, 2702–2706. doi:10.1021/jf00058a028

705 Carbonell-Alcaina, C., Corbatón-Báguena, M.-J., Alvarez-Blanco, S., Bes-Piá, M.A.,  
706 Mendoza-Roca, A., Pastor-Alcañiz, L., 2016. Determination of fouling  
707 mechanisms in polymeric ultrafiltration membranes using residual brines from  
708 table olive storage wastewaters as feed. *J. Food Eng.* 187, 14–23.  
709 doi:10.1016/j.jfoodeng.2016.04.016

710 Cassano, A., Conidi, C., Drioli, E., 2011. Comparison of the performance of UF

711 membranes in olive mill wastewaters treatment. *Water Res.* 45, 3197–3204.  
712 doi:10.1016/j.watres.2011.03.041

713 Cassano, A., Conidi, C., Giorno, L., Drioli, E., 2013. Fractionation of olive mill  
714 wastewaters by membrane separation techniques. *J. Hazard. Mater.* 248-249, 185–  
715 193. doi:10.1016/j.jhazmat.2013.01.006

716 Cheryan, M., 1998. *Ultrafiltration and Microfiltration Handbook*, Taylor&Francis  
717 Routledge. doi:97-62251

718 Coskun, T., Debik, E., Demir, N.M., 2010. Treatment of olive mill wastewaters by  
719 nanofiltration and reverse osmosis membranes. *Desalination* 259, 65–70.  
720 doi:10.1016/j.desal.2010.04.034

721 De Castro, A., Brenes, M., 2001. Fermentation of washing waters of spanish-style green  
722 olive processing. *Process Biochem.* 36, 797–802. doi:10.1016/S0032-  
723 9592(00)00280-6

724 El-Abbassi, A., Khayet, M., Hafidi, A., 2011. Micellar enhanced ultrafiltration process  
725 for the treatment of olive mill wastewater. *Water Res.* 45, 4522–4530.  
726 doi:10.1016/j.watres.2011.05.044

727 El-Abbassi, A., Kiai, H., Raiti, J., Hafidi, A., 2014. Application of ultrafiltration for  
728 olive processing wastewaters treatment. *J. Clean. Prod.* 65, 432–438.  
729 doi:10.1016/j.jclepro.2013.08.016

730 Fendri, I., Chamkha, M., Bouaziz, M., Labat, M., Sayadi, S., Abdelkafi, S., 2013. Olive  
731 fermentation brine: biotechnological potentialities and valorization. *Environ.*  
732 *Technol.* 34, 181–193. doi:10.1080/09593330.2012.689364

733 Ferrer-Polonio, E., Mendoza-Roca, J. A., Iborra-Clar, A., Pastor-Alcañiz, L., 2014.  
734 Fermentation brines from Spanish style green table olives processing: treatment

735 alternatives previous to recycling or recovery operations. *J. Chem. Technol.*  
736 *Biotechnol.* doi:10.1002/jctb.4550

737 Ferrer-Polonio, E., Mendoza-Roca, J.A., Iborra-Clar, A., Alonso-Molina, J.L., Pastor-  
738 Alcañiz, L., 2015. Comparison of two strategies for the start-up of a biological  
739 reactor for the treatment of hypersaline effluents from a table olive packaging  
740 industry. *Chem. Eng. J.* 273, 595–602. doi:10.1016/j.cej.2015.03.062

741 Field, R.W., Pearce, G.K., 2011. Critical, sustainable and threshold fluxes for  
742 membrane filtration with water industry applications. *Adv. Colloid Interface Sci.*  
743 164, 38–44. doi:10.1016/j.cis.2010.12.008

744 Field, R.W., Wu, D., Howell, J.A., Gupta, B.B., 1995. Critical flux concept for  
745 microfiltration fouling. *J. Memb. Sci.* 100, 259–272.

746 Garcia-Castello, E., Cassano, A., Criscuoli, A., Conidi, C., Drioli, E., 2010. Recovery  
747 and concentration of polyphenols from olive mill wastewaters by integrated  
748 membrane system. *Water Res.* 44, 3883–3892. doi:10.1016/j.watres.2010.05.005

749 García-García, P., López-López, A., Moreno-Baquero, J.M., Garrido-Fernández, A.,  
750 2011. Treatment of wastewaters from the green table olive packaging industry  
751 using electro-coagulation. *Chem. Eng. J.* 170, 59–66.  
752 doi:10.1016/j.cej.2011.03.028

753 Garrido, A., García, P., Brenes, M., 1992. The recycling of table olive brine using  
754 ultrafiltration and activated carbon adsorption. *J. Food Eng.* 17, 291–305.  
755 doi:10.1016/0260-8774(92)90046-9

756 Guedes, A.C., Amaro, H.M., Malcata, F.X., 2011. Microalgae as sources of high added-  
757 value compounds-a brief review of recent work. *Biotechnol. Prog.* 27, 597–613.  
758 doi:10.1002/btpr.575

759 Ho, C., Zydney, A.L., 2000. A combined pore blockage and cake filtration model for  
760 protein fouling during microfiltration. *J. Colloid Interface Sci.* 232, 389–399.  
761 doi:10.1006/jcis.2000.7231

762 International Olive Council, 2015. Total produced worldwide table olives by country.  
763 Compiled data taken from: <http://www.internationaloliveoil.org>.

764 Kargı, F., Dinçer, A.R., 1999. Salt inhibition effects in biological treatment of saline  
765 wastewater in RBC. *J. Environ. Eng.* 125, 966–971.

766 Kiai, H., García-Payo, M.C., Hafidi, A., Khayet, M., 2014. Application of membrane  
767 distillation technology in the treatment of table olive wastewaters for phenolic  
768 compounds concentration and high quality water production. *Chem. Eng. Process.*  
769 86, 153–161. doi:10.1016/j.cep.2014.09.007

770 Kiai, H., Hafidi, A., 2014. *LWT - Food Science and Technology* Chemical composition  
771 changes in four green olive cultivars during spontaneous fermentation. *Food Sci.*  
772 *Technol.* 57, 663–670. doi:10.1016/j.lwt.2014.02.011

773 Lefebvre, O., Moletta, R., 2006. Treatment of organic pollution in industrial saline  
774 wastewater: A literature review. *Water Res.* 40, 3671–3682.  
775 doi:10.1016/j.watres.2006.08.027

776 Luján-Facundo, M.J., Mendoza-Roca, J.A., Cuartas-Urbe, B., Álvarez-Blanco, S.,  
777 2015. Evaluation of cleaning efficiency of ultrafiltration membranes fouled by  
778 BSA using FTIR – ATR as a tool. *J. Food Eng.* 163, 1–8.  
779 doi:10.1016/j.jfoodeng.2015.04.015

780 Mondal, S., Chhaya, De, S., 2012. Prediction of ultrafiltration performance during  
781 clarification of stevia extract. *J. Memb. Sci.* 396, 138–148.  
782 doi:10.1016/j.memsci.2012.01.009

783 Paraskeva, C. a., Papadakis, V.G., Tsarouchi, E., Kanellopoulou, D.G., Koutsoukos,  
784 P.G., 2007. Membrane processing for olive mill wastewater fractionation.  
785 Desalination 213, 218–229. doi:10.1016/j.desal.2006.04.087

786 Parinos, C.S., Stalikas, C.D., Giannopoulos, T.S., Pilidis, G. a., 2007. Chemical and  
787 physicochemical profile of wastewaters produced from the different stages of  
788 Spanish-style green olives processing. J. Hazard. Mater. 145, 339–343.  
789 doi:10.1016/j.jhazmat.2006.12.061

790 Pereira, J.A., Pereira, A.P.G., Ferreira, I.C.F.R., Valentão, P., Andrade, P.B., Seabra, R.,  
791 Etevinho, L., Bento, A., 2006. Table olives from Portugal: Phenolic compounds,  
792 antioxidant potential, and antimicrobial activity. J. Food Agric. Food Chem. 54,  
793 8425–8431.

794 Reid, E., Liu, X., Judd, S.J., 2006. Effect of high salinity on activated sludge  
795 characteristics and membrane permeability in an immersed membrane bioreactor.  
796 J. Memb. Sci. 283, 164–171. doi:10.1016/j.memsci.2006.06.021

797 Rivas, F.J., Beltrán, F.J., Gimeno, O., Alvarez, P., 2003. Treatment of brines by  
798 combined Fenton's reagent-aerobic biodegradation II. Process modelling. J.  
799 Hazard. Mater. 96, 259–276. doi:10.1016/S0304-3894(02)00216-9

800 Ryan, D., Robards, K., Lavee, S., 1999. Changes in phenolic content of olive during  
801 maturation. Int. J. Food Sci. Technol. 34, 265–274.

802 Sánchez Gómez, A.H., García García, P., Rejano Navarro, L., 2006. Trends in table  
803 olive production: Elaboration of table olives. Grasas y Aceites 57, 86–94.  
804 doi:10.3989/gya.2006.v57.i1.24

805 Sánchez-Moreno, C., Plaza, L., de Ancos, B., Cano, M.P., 2006. Nutritional  
806 characterisation of commercial traditional pasteurised tomato juices: carotenoids,

807 vitamin C and radical-scavenging capacity. *Food Chem.* 98, 749–756.  
808 doi:10.1016/j.foodchem.2005.07.015

809 Singleton, V.L., Orthofer, R., Lamuela-Raventós, R.M., 1999. Analysis of total phenols  
810 and other oxidation substrates and antioxidants by means of folin-ciocalteu  
811 reagent. *Methods Enzymol.* 299, 152–178. doi:10.1016/S0076-6879(99)99017-1

812 Soler-Rivas, C., Espiñ, J.C., Wichers, H.J., 2000. Oleuropein and related compounds. *J.*  
813 *Sci. Food Agric.* 80, 1013–1023. doi:10.1002/(SICI)1097-  
814 0010(20000515)80:7<1013::AID-JSFA571>3.0.CO;2-C

815 Tripoli, E., Giammanco, M., Tabacchi, G., Di Majo, D., Giammanco, S., La Guardia,  
816 M., 2005. The phenolic compounds of olive oil: structure, biological activity and  
817 beneficial effects on human health. *Nutr. Res. Rev.* 18, 98–112.  
818 doi:10.1079/NRR200495

819 Ulbricht, M., Ansorge, W., Danielzik, I., König, M., Schuster, O., 2009. Fouling in  
820 microfiltration of wine: The influence of the membrane polymer on adsorption of  
821 polyphenols and polysaccharides. *Sep. Purif. Technol.* 68, 335–342.  
822 doi:10.1016/j.seppur.2009.06.004

823 Vatanpour, V., Esmaeili, M., Hossein, M., Abadi, D., 2014. Fouling reduction and  
824 retention increment of polyethersulfone nano filtration membranes embedded by  
825 amine-functionalized multi-walled carbon nanotubes. *J. Memb. Sci.* 466, 70–81.  
826 doi:10.1016/j.memsci.2014.04.031

827 Woolard, C.R., Irvine, R.L., 1994. Biological treatment of hypersaline wastewater by a  
828 biofilm of halophilic bacteria. *Water Environ. Res.* 66, 230–235.

829 Zagklis, D.P., Vavouraki, A.I., Kornaros, M.E., Paraskeva, C. A., 2015. Purification of  
830 olive mill wastewater phenols through membrane filtration and resin

831 adsorption/desorption. J. Hazard. Mater. 285, 69–76.  
832 doi:10.1016/j.jhazmat.2014.11.038

833 Zirehpour, A., Rahimpour, A., Jahanshahi, M., 2015. The filtration performance and  
834 efficiency of olive mill wastewater treatment by integrated membrane process.  
835 Desalin. Water Treat. 53, 1254–1262. doi:10.1080/19443994.2013.855884

836 Zulueta, A., Esteve, M.J., Frasquet, I., Frígola, A., 2007. Vitamin C, vitamin A,  
837 phenolic compounds and total antioxidant capacity of new fruit juice and skim  
838 milk mixture beverages marketed in Spain. Food Chem. 103, 1365–1374.  
839 doi:10.1016/j.foodchem.2006.10.052

840